

Dynamic screening in $L_{2,3}$ -shell transition metal x-ray absorption

A. L. Ankudinov, A. I. Nesvizhskii,* and J. J. Rehr

Dept. of Physics, Box 351560, University of Washington, Seattle, Washington 98195

(Dated: November 21, 2018)

Abstract

Calculations of L -shell x-ray absorption in transition metals are shown to be sensitive to screening, both of the x-ray field and the photoelectron-core hole interaction. This screening is calculated using a generalization of the time dependent local density approximation and a projection onto a local atomic basis. The approach yields renormalized dipole-matrix elements which account for the observed deviations of the L_3/L_2 branching ratio from the 2:1 value of independent electron theory.

PACS numbers: 78.70.Dm, 78.20.Ls, 75.50.Cc

arXiv:cond-mat/0203097v1 [cond-mat.mtrl-sci] 5 Mar 2002

*now at Institute for Systems Biology, Seattle WA 98103

Independent-electron theory is generally successful in describing near edge x-ray absorption spectra (XAS) [1]. However, it fails dramatically at the $L_{2,3}$ edges in 3d transition metals [2, 3, 4, 5]. While the independent electron approximation predicts an L_3/L_2 transition intensity “branching ratio” close to 2:1, the observed ratio (Fig. 1) varies considerably with respect to atomic number Z , and is closer to 1:1 for metals like Ti and V with nearly empty d -bands [6, 7, 8]. This puzzling behavior is thought to reflect many-body effects due to the Coulomb interaction, but despite many studies, its variation has never been quantitatively explained. We now show, however, that the observed branching-ratio depends crucially on dynamic screening of the x-ray field and the photoelectron–core hole interaction, and can be calculated using a simplified dynamic screening model and a generalization of the time-dependent local density approximation (TDLDA). Our approach makes use of a projection onto a local atomic basis and a real-space multiple-scattering (RSMS) formalism [9]. This yields an efficient matrix formulation for extended systems, yet retains the simplicity of the TDLDA, and gives results in good agreement with experiment.

The $L_{2,3}$ XAS corresponds to transitions from the $2p_{1/2}$ and $2p_{3/2}$ levels to continuum s and d states. Several many body effects can be identified which contribute to a non-constant L_3/L_2 intensity branching ratio: i) Inelastic losses – these can be represented in terms of lifetime and self-energy effects in independent-electron calculations. The lifetimes are different for the L_2 and L_3 edges due to the Coster-Kronig mechanism [10], but this difference only increases the branching ratios, e.g., to about 3:1. ii) Dynamic core polarization – i.e., the creation of local fields which screen the external x-ray field. This polarization effect may be treated [5, 11] within the TDLDA by neglecting exchange terms, an approximation often referred to as the random phase approximation (RPA). This leads to a considerable reduction of the branching ratio, but does not account well for its variation with Z . iii) Screening of the photoelectron-core hole interaction – this effect, which we find to be crucial, can be addressed in terms of a frequency dependent exchange-correlation kernel $f_{xc}(\omega)$ in the TDLDA [12], or by the analogous, non-local dynamically screened particle-hole interaction in the Bethe-Salpeter equation (BSE) [13, 14, 15, 16]. The importance of dynamic screening of the core-hole is surprising, since it has been argued variously that corrections to the RPA are small [5, 11], or that an adiabatic kernel f_{xc}^0 is often adequate [11, 12].

The TDLDA [5, 11, 17] provides an efficient formalism for calculations of response functions, including corrections to the independent electron approximation, since it avoids the

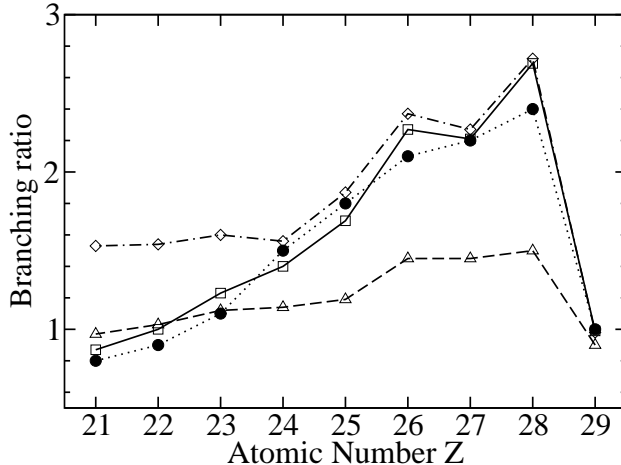


FIG. 1: L_3/L_2 intensity branching ratio for the transition metal series from experiment (solid circles), and as calculated with different exchange correlation kernels: RPA (triangles), adiabatic f_{xc}^0 (diamonds); and the dynamic model of this work (see text) $\tilde{f}_{xc}(\tilde{\omega})$ (squares).

complications of non-locality in the time-dependent Hartree-Fock (TDHF) [18], BSE, or configuration interaction approaches. The TDLDA was originally introduced for atoms [11], but has since been extended to many other systems [17] including band-structure formulations for transition metals [5]. The TDLDA and TDHF equations are closely similar to the BSE [13, 14, 15, 16], which provides a systematic, many-body framework based on the 2-particle Green's function for treating core-hole screening. The crucial difference between the TDLDA and the BSE lies in the structure of the exchange-correlation kernel $f_{xc}(\omega)$; in addition the single-particle states are replaced by quasiparticle states which take the electron self-energy into account. Our approach (see below) is an extension of the TDLDA derived in part from the BSE. Like the BSE, our approach also uses a quasiparticle approximation for single-particle states, with inelastic losses approximated by a Hedin-Lundqvist electron-gas self energy [19]. Such losses are crucial in XAS and also point to the importance of dynamic screening. Our method simplifies the screening calculations by using a local basis. Local basis set methods have also been used to advantage in various related calculations [20, 21].

Within the TDLDA [11] or TDHF [18] approximations, the photon cross-section (or XAS) $\sigma(\omega)$ can be expressed as an integral over the non-interacting response function $\chi_0(\vec{r}, \vec{r}', \omega)$ and the screened x-ray field $\phi(\vec{r}, \omega)$. For notational simplicity, it is convenient to regard the continuous coordinates \vec{r} and \vec{r}' as vector or matrix indices, which may be suppressed unless

needed for clarity. Then the XAS can be expressed compactly as

$$\sigma(\omega) = -\frac{4\pi\omega}{c}\phi^*(\omega)[\text{Im } \chi_0(\omega)]\phi(\omega), \quad (1)$$

where

$$\chi_0(\vec{r}, \vec{r}', \omega) = \sum_{ij} (f_i - f_j) \frac{\psi_i^*(\vec{r})\psi_i(\vec{r}')\psi_j^*(\vec{r}')\psi_j(\vec{r})}{\omega + E_i - E_j + i0^+}. \quad (2)$$

Eq. (1) is equivalent to an analogous expression with ϕ replaced by the external x-ray field ϕ^{ext} and χ_0 by the full response function χ [11]. Here f_i are Fermi occupation numbers (1 or 0), and the sums run over all one-electron eigenstates $\psi_i(\vec{r})$ of the ground state Hamiltonian. The field $\phi(\omega)$ consists of the external field $\phi^{ext} \equiv \hat{\epsilon} \cdot \vec{r}$ (in the dipole approximation) plus an induced local field, which in matrix form is given by

$$\phi(\omega) = \epsilon^{-1}(\omega)\phi^{ext}(\omega), \quad \epsilon(\omega) = 1 - K(\omega)\chi^0(\omega). \quad (3)$$

Here $K(\vec{r}, \vec{r}', \omega)$ denotes the particle-hole interaction (or TDLDA kernel), which contains direct and exchange parts, i.e.,

$$K(\vec{r}, \vec{r}', \omega) = V(\vec{r}, \vec{r}') + f_{xc}(\vec{r}, \vec{r}', \omega), \quad (4)$$

and $V = 1/|\vec{r} - \vec{r}'|$ is the Coulomb interaction.

In this paper we consider several approximations for $f_{xc}(\omega)$, which is generally a non-local, frequency dependent operator: i) The RPA ($f_{xc} = 0$) – to the extent exchange can be neglected, the RPA is adequate [5]. ii) Adiabatic TDLDA ($f_{xc}(0) = f_{xc}^0$) – this static limit $f_{xc}^0(\vec{r}, \vec{r}') = \delta(\vec{r} - \vec{r}')\delta v_{xc}[\rho(\vec{r})]/\delta\rho$, is dependent on the local density and is obtained from the ground-state LDA exchange-correlation potential $v_{xc}[\rho]$. iii) Dynamic TDLDA model – An LDA for the frequency dependence of $f_{xc}(\omega)$ was developed by Gross and Kohn [12]. At the large x-ray energies of interest here, this $f_{xc}(\omega)$ is strongly suppressed, and yields results close to the RPA [5]. However, such results are clearly at odds with experiment for nearly empty d -bands (Fig. 1). iv) Dynamic TDLDA/BSE model – Our aim here is to improve on i), ii) and iii) for $L_{2,3}$ XAS, based partly on the BSE [13, 14, 15, 16]. In the BSE, the matrix elements $\langle vc|f_{xc}(\omega)|v'c' \rangle$ depend on the dynamically screened Coulomb interaction $W(\omega) = \tilde{\epsilon}^{-1}(\omega)V$, through an effective inverse dielectric matrix $\tilde{\epsilon}^{-1}(\omega)$ [15]. However the actual dependence on $\omega \approx E_c - E_v$ is matrix element dependent, and depends on the effective dielectric response at the energy-transfer frequency, i.e., $\tilde{\omega} = \omega + E_{c'} - E_v \approx E_{v'} - E_v$. This behavior can be seen

explicitly in plasmon-pole models [13]. For $L_{2,3}$ XAS, the most important occupied states v, v' are the $2p_{1/2}$ and $2p_{3/2}$ levels, which are split by a moderate spin-orbit interaction Δ_{so} , ranging from 5 eV for Sc to 20 eV for Cu. The matrix elements with zero energy transfer correspond to static screening; thus it is reasonable to set $f_{xc}(\omega) = f_{xc}^0$ for $v = v'$. We also tried the unscreened, non-local TDHF exchange operator for $v = v'$, which corresponds to an unscreened core-hole potential, but found it to be much too strong. For the off-diagonal elements ($v \neq v'$), however, we found that the unscreened exchange operator (i.e., the high frequency limit $W = V$) has only a small effect. This suggests that the effects of dynamic screening on off-diagonal terms at moderately high frequency $\tilde{\omega} = \Delta_{so}$ are also small and can be neglected. This behavior is in contrast to the case for optical absorption, where the adiabatic limit ($\tilde{\omega} = 0$) is a good approximation and can be used for all matrix elements [13]. Thus remarkably, we find that elaborate calculations of dynamical screening can be avoided for $L_{2,3}$ XAS by using a simplified dynamic model $f_{xc}(\omega) \rightarrow \tilde{f}_{xc}(\tilde{\omega})$, $\tilde{\omega} = E_v - E_{v'}$, i.e., $\tilde{f}_{xc}(\tilde{\omega}) = f_{xc}^0$ for $\tilde{\omega} = 0$ and $\tilde{f}_{xc}(\tilde{\omega}) = 0$, ($\tilde{\omega} = \Delta_{so}$) This defines our dynamic TDLDA/BSE model, which leads to reasonable agreement with experiment (Fig. 1).

Next we briefly outline our calculations, which make use of the RSMS formalism (i.e., the real-space analog of the Korringa-Kohn Rostoker (KKR) band structure method) of our self-consistent, all-electron FEFF8 code [9]. To begin we rewrite Eq. (1) as

$$\sigma(\omega) = \frac{4\pi e^2 \omega}{c} \sum_{v, LL'} \tilde{M}_{vL}(\omega) \rho_{L, L'}(E) \tilde{M}_{vL'}(\omega), \quad (5)$$

where $E = \omega + E_v - E_F$ is the photoelectron energy. The screening of both the x-ray field and the photoelectron-core hole interaction are included implicitly in the renormalized dipole matrix elements [18], $\tilde{M}_{vL}(\omega) = \langle R_L | \phi | v \rangle$, where $L = (\kappa, m)$ denotes a relativistic angular momentum basis. The quantities $\rho_{L, L'}(E)$ are matrix elements of the unoccupied one-electron density matrix,

$$\begin{aligned} \rho(\vec{r}, \vec{r}', E) &\equiv \sum_c \psi_c(\vec{r}) \psi_c^*(\vec{r}') \delta(E - E_c), \\ &= \sum_{L, L'} R_L(\vec{r}) R_{L'}(\vec{r}') \rho_{L, L'}(E), \\ \rho_{L, L'}(E) &= \delta_{L, L'} + \chi_{L, L'}(E). \end{aligned} \quad (6)$$

Here $R_L(\vec{r}, E)$ are normalized scattering states calculated with the absorbing atom potential, and $\chi_{L, L'}(E)$ contains the fine structure in the XAS due to scattering by the environment

[9]. Note that by replacing ϕ with ϕ^{ext} in Eq. (5), the screened dipole matrix elements \tilde{M}_{vL} become bare dipole matrix elements $M_{vL} = \langle R_L | \hat{\epsilon} \cdot \vec{r} | i \rangle$, and one recovers the independent electron formula, equivalent to Fermi's Golden Rule. Since the strength of the XAS is a measure of the screening response, the independent-electron approximation should become increasingly valid away from the edge region.

The second key approximation in our approach is the use of a local basis for calculations of χ_0 and \tilde{M}_{vL} . This is done starting from an expression in terms of a Kramers-Kronig (KK) transform over the density matrix,

$$\chi_0(\vec{r}, \vec{r}', \omega) = \sum_v \psi_v^*(\vec{r}) \psi_v(\vec{r}') \int_{E_F}^{\infty} \frac{dE}{\pi} \rho(\vec{r}, \vec{r}', E) \times \left[\frac{1}{\omega - E + E_v + i\delta} + \frac{1}{\omega + E - E_v + i\delta} \right]. \quad (7)$$

Once χ_0 is known, Eq. (3) could be solved iteratively in real space to obtain $\phi(\vec{r})$ [11]. However, this procedure is computationally expensive for extended systems, since it involves KK transforms for many $(\vec{r}, \vec{r}', \omega)$ points. To simplify this calculations, we make the reasonable assumption [11] that the induced charge $\rho^{ind} = \chi_0(\omega)\phi$ that screens the x-ray field, is local and arises largely from a few significant orbitals on the absorbing atom. This is convenient, since our formulation only needs the screened field $\phi(\vec{r}, \omega)$ at short distances to calculate the deep-core transition matrix $\tilde{M}_{vL}(\omega)$. Thus to approximate ϕ , we introduce the atomic projection operator $P = \sum_n |\psi_n\rangle\langle\psi_n|$, which projects a given function onto a local basis set of atomic-like orbitals on the central atom. Then the density matrix can be approximated by its local contribution $\rho \approx \rho^{loc} = P\rho P$. These approximations can be systematically improved by including a more complete set. Thus

$$\chi_0^{loc}(\vec{r}, \vec{r}', \omega) = \sum_{vnn'} \psi_v^*(\vec{r}) \psi_n^*(\vec{r}') \chi_{vn, vn'}^{loc}(\omega) \times \psi_v(\vec{r}') \psi_{n'}(\vec{r}), \quad (8)$$

$$\chi_{vn, vn'}^{loc}(\omega) = -\frac{k}{\pi} \sum_{L, L'} \int_{E_F}^{\infty} dE \frac{\langle n | R_L \rangle \rho_{L, L'} \langle R_{L'} | n' \rangle}{\omega - E + E_v + i\delta},$$

where $k = \sqrt{2(\omega + E_v)}$. Note that the localized part of χ_0 does not require a KK transform at each point, since the localized part of the photoelectron wave function can be separated into energy and position dependent parts. Moreover, the overlap matrices $\langle n | R_L \rangle$ decay rapidly with energy, so the KK transform converges well. This approximation then leads to a fast matrix formulation for \tilde{M}_{vL} . From Eq. (3), we obtain (summation over repeated

indices being implicit)

$$\begin{aligned} \phi(\vec{r}, \omega) &\approx \phi^{ext}(\vec{r}, \omega) + \sum_{v'n'n''} \int d\vec{r}' K(\vec{r}, \vec{r}', \omega) \\ &\times \psi_{v'}^*(\vec{r}') \psi_{n'}(\vec{r}') \chi_{v'n',v'n''}^0(\omega) \tilde{M}_{v'n''}, \end{aligned} \quad (9)$$

where $\tilde{M}_{vn} = \langle \psi_n | \phi | v \rangle$ is calculated by integrating Eq. (9) over the core and basis set functions,

$$\begin{aligned} \tilde{M}_{vn}(\omega) &= M_{vn} + K_{vn,v'n'} \tilde{\chi}_{v'n',v'n''}^{loc}(\omega) \tilde{M}_{v'n''}(\omega), \\ M_{vn} &= \langle n | \phi^{ext} | v \rangle, \quad K_{vn,v'n'} = \langle vn | K | v'n' \rangle. \end{aligned} \quad (10)$$

These equations can readily be solved by matrix inversion. Finally on integrating Eq. (9) over the core- and final state-wave functions, we get

$$\begin{aligned} \tilde{M}_{vL}(\omega) &= M_{vL}(\omega) + K_{vL,v'n'} \chi_{vn',v'n''}^{loc} \tilde{M}_{v'n''}, \\ K_{vL,v'n'} &= \langle vR_L | K(\omega) | v'n' \rangle, \end{aligned} \quad (11)$$

where R_L denotes the scattering-state $R_L(\omega - E_v)$. The matrix form in Eq. (11) is very efficient, and has been implemented using an extension of our FEFF8 code. This extension is straightforward, since only the dipole matrix elements need be modified to incorporate screening. Due to the local form of $\tilde{f}_{xc}(\tilde{\omega})$, the contributions to $K_{vL,v'n'}(\omega)$ satisfy the same selection rules and can be calculated using standard formulas for Coulomb interaction matrix elements [22].

Typical results near the beginning and end of the transition metal series are presented for Ti and Ni in Fig. 2. The dramatic differences reflect differences in the response between nearly empty and nearly filled d -bands, and are strongly dependent on the form of $f_{xc}(\omega)$. For all calculations we used theoretical atomic core-hole life-times [10]. We did not add additional broadening to correct for experimental resolution, though this would give slightly better agreement with experiment (Fig. 1). Our results for the RPA agree well with those of Ref. [5], which validates our local screening approximation. Note that the RPA is only a good approximation for nearly empty d -bands, while the adiabatic f_{xc}^0 is appropriate only for nearly filled ones. However, our dynamic model $\tilde{f}_{xc}(\tilde{\omega})$ is clearly satisfactory for the entire series.

Since screening redistributes the oscillator strength between the L_2 and L_3 edges, the importance of these many-body corrections appears to cast doubt on the accuracy of results

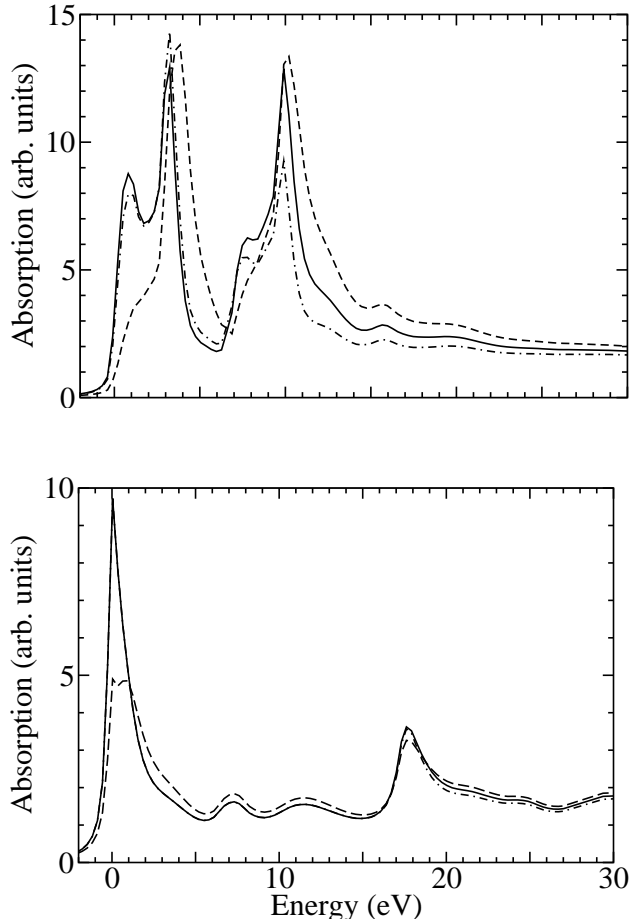


FIG. 2: $L_{3,2}$ edge XAS vs energy with respect to the Fermi level, for a) Ti (upper figure) and b) Ni (lower), as calculated with different screening models: RPA (solid), static fxc^0 (dots), and the dynamic model of this work $\tilde{f}_{xc}(\omega)$ (dashes).

obtained from the XAS “sum-rules” [5]. These sum-rules allow one to determine various spin- and orbital-moments from linear combinations of the L_2 and L_3 XAS [23]. However, one can now correct these procedures for local-field effects with our approach, e.g., by substituting the screened XAS cross-section, in place of the one-electron result in the analysis.

In summary, we have found that dynamic screening of the photoelectron-core hole interaction, which gives rise to a frequency dependent exchange-correlation operator $f_{xc}(\omega)$, is crucial in calculations of transition metal $L_{2,3}$ spectra. However, we have found a dynamic model based on the TDLDA and BSE, which accounts well for the frequency and matrix element dependence, by neglecting off diagonal, high frequency screening terms. With this model, we have developed an efficient approach for including screening in deep-core XAS,

based on calculations of screened dipole matrix elements. Our approach goes beyond the conventional TDLDA, and is similar in some respects to a screened TDHF approximation [16]. Moreover, the approach yields good agreement with experiment for the $L_{2,3}$ XAS of 3d transition metals, without the complexity of full dynamic-screening calculations.

Acknowledgments

We thank J. Chelikowsky, H. Ebert, W. Ku, Z. Levine, S. Pantelides, G. Sawatzky, E. Shirley and especially G. Bertsch and A. Soininen for helpful comments. This work was supported by DOE grants DE-FG03-97ER45623 and DE-FG03-98ER45718, and was facilitated by the DOE Computational Materials Science Network.

-
- [1] J. J. Rehr and R. C. Albers, *Rev. Mod. Phys.* **72**, 621 (2000).
 - [2] J. Zaanen, G. A. Sawatzky, J. Fink, W. Speier and J. C. Fuggle, *Phys. Rev. B* **32**, 4905 (1985).
 - [3] W. G. Waddington, P. Rez, I. P. Grant and C. J. Humphreys, *Phys. Rev. B* **34**, 1467 (1986).
 - [4] B. T. Thole and G. van der Laan, *Phys. Rev. B* **38**, 3158 (1988).
 - [5] J. Schwitalla and H. Ebert, *Phys. Rev. Lett.* **80**, 4586 (1998).
 - [6] R. D. Leapman and L. A. Grunes, *Phys. Rev. Lett.* **45**, 397 (1980); R. D. Leapman, L. A. Grunes, and P. L. Fejes, *Phys. Rev. B* **26**, 614 (1982).
 - [7] J. Fink, Th. Müller-Heinzerling, B. Scheerer, W. Speier, F. U. Hillebrecht, J. C. Fuggle, J. Zaanen, and G. A. Sawatzky, *Phys. Rev. B* **32**, 4899 (1985).
 - [8] J. Barth, F. Gerken, and C. Kunz, *Phys. Rev. B* **28**, 3608 (1983).
 - [9] A. L. Ankudinov, B. Ravel, J. J. Rehr, and S. D. Conradson, *Phys. Rev. B* **58**, 7565 (1998).
 - [10] O. Keski-Rankonen and M. O. Krause, *At. Data and Nuc. Dat. Tab.* **14**, 139 (1974).
 - [11] A. Zangwill and P. Soven, *Phys. Rev. A* **21** 1561, (1980); A. Zangwill and Liberman, *J. Phys. B: At. Mol. Phys.* **17**, L253 (1984).
 - [12] E. K. U. Gross, and W. Kohn, *Adv. Quantum Chem.* **21**, 255 (1990).
 - [13] M. Rohlfing and S. G. Louie, *Phys. Rev. B* **62**, 4927 (2000).
 - [14] J. A. Soininen and E. L. Shirley, *Phys. Rev. B* **64**, 165112 (2001).
 - [15] G. Strinati, *Phys. Rev. B* **29**, 5718 (1984).

- [16] W. Hanke and L. J. Sham, Phys. Rev. B **21**, 4656 (1980).
- [17] See for example, G. F. Bertsch, J.-I. Iwata, A. Rubio, and K. Yabana, Phys. Rev. B **62**, 7998 (2000); I. Vasiliev, S. Ögut and J. Chelikowsky, Phys. Rev. Lett. **82**, 1919 (1999).
- [18] Z. Crljen and G. Wendin, Phys. Rev. A **35**, 1555 (1987).
- [19] B. I. Lundqvist, Phys. Kondens. Materie **6**, 193 (1967).
- [20] F. Aryasetiawan and O. Gunnarsson, Phys. Rev. Lett. **74**, 3221 (1995).
- [21] M. Rohlfing, P. Krüger and J. Pollmann, Phys. Rev. B **48**, 17791 (1993).
- [22] I. P. Grant, Adv. Phys. **19**, 747 (1970).
- [23] A. I. Nesvizhskii, A. L. Ankudinov and J. J. Rehr, Phys. Rev. B **63**, 094412 (2001); A. L. Ankudinov, A. I. Nesvizhskii and J. J. Rehr, J. Synchrotron Rad. **8**, 92 (2001).